An Unprecedented Incident of Concrete Contamination by Marine Deposits in Bored Pile Construction Leading to Abandonment of the Piles in a Hong Kong Building Project

Thomas S.K. Lam
Wilson & Associates Limited, Hong Kong

doi: https://doi.org/10.21467/proceedings.8.2.11

ABSTRACT

In a building project constructed on Hong Kong Island near the seashore, bored piles of 1.5 m and 2.0 m in diameter founded on Grade III or better rock were used as foundation for the building. The site is underlain by fill, marine deposits, alluvium, completely decomposed granite and moderately to slightly decomposed granite. In the concreting of two bored piles, a sudden drop of some 4.7 m and 6.5 m in the concrete level in the temporary casing was noted, as the casing was lifted. In both piles, it was suspected that a hardened concrete layer was formed in the piles during concreting. These two piles were abandoned in the end. An investigation was carried out. Taking into account of the new information obtained, it was established that there was concrete contamination by marine deposits at the casing toe level upon lifting of the casing, leading to early setting of concrete and formation of a hardened concrete layer in the piles. In this paper, the concreting problem encountered in the two piles and the new information obtained are presented. The mechanism of concrete contamination by marine deposits, leading to early setting of concrete and formation of a hardened concrete layer in the piles, is given.

1 INTRODUCTION

In a building project constructed on Hong Kong Island near the seashore, bored piles of 1.5 m and 2.0 m in diameter founded on Grade III or better rock are used as foundation for the building. The site is underlain by fill, marine deposits, alluvium, completely decomposed granite and moderately to slightly decomposed granite. In the construction of the bored piles, a temporary casing was first oscillated into the ground at the pile location. After the casing was installed, the materials inside the casing were excavated using a hammer grab. Throughout the excavation, water level inside the casing was checked to ensure that it was above the groundwater level in the vicinity. The installation of casing and excavation were carried out in sequence with the excavation carried out in at least 2 m above the casing toe. When the bedrock was reached, reverse circulation drilling was used to form the rock socket. A minimum socket of 500 mm in rock was provided for the casing. The concrete used for the piles (a grade 45D/20PFA concrete was used) was placed under water by a tremie pipe. An immersion of at least 2 m of the tremie pipe in the concrete was maintained during concreting.

In the concreting of two bored piles (BP30 and BP9), which are 59.23 m and 63.50 m long respectively, a sudden and significant drop of concrete level in the casing was noted, as the casing was lifted. In BP30, the concrete dropped by 4.7 m from 14.9 m to 19.6 m depth, which failed to rise even after adding a further five loads of concrete of 37.5 m^3, followed by lifting of the casing. In BP9, the concrete dropped by 6.5 m from 19.1 m to 25.6 m depth. There was difficulty to re-insert the tremie pipe back into the concrete at 28.0 m depth after it was lifted. In both piles, it was suspected that a hardened concrete layer was formed in the piles during concreting. These two piles were abandoned in the end.

An investigation was carried out, which included completion of four additional drillholes, installation of vibrating wire (VW) piezometers in the drillholes to continuously monitor the groundwater level fluctuation, determination of the composition and contents of the affected concrete in the piles by Particle Size Distribution (PSD), X-ray Diffraction (XRD) and X-ray Fluorescence (XRF) tests, testing of groundwater for dissolved carbon dioxide (CO_2) and marine deposits for organic matter, etc. Taking into account of the new information obtained, it was established that there was concrete contamination by marine deposits at the casing toe level upon lifting of the casing, leading to early setting of concrete and formation of a hardened concrete layer in the piles.

© 2026 Copyright held by the author(s). Published by AIJR Publisher in " Proceedings of The HKIE Geotechnical Division 46th Annual Seminar 2026: Bridging Theory and Practice in Geotechnical Engineering" (GDAS2026). Organized by the Geotechnical Division, The Hong Kong Institution of Engineers, Hong Kong on May 12, 2026.

Proceedings DOI: 10.21467/proceedings.8.2; Series: AIJR Proceedings; ISSN: 2582-3922; ISBN: 978-81-688301-1-0

In this paper, the concreting problem encountered in the two piles during construction and the new information obtained from the investigation are presented. A detailed description of the mechanism of concrete contamination by marine deposits, leading to early setting of concrete and formation of a hardened concrete layer in the piles, is given.

2 TENDER GI WORKS

2.1 Ground Conditions

A total of 9 drillholes (DH1, DH2, DH3, DH4, DH6, DH7, DH8, DH9 and DH10) were completed. Location of the drillholes is shown in Figure 1. Location of BP30 and BP90 is also included. The geological profile of the site based on the tender GI information along Section C-C' is shown in Figure 2.

The site is underlain by fill, marine deposits, alluvium, completely decomposed granite (CDG) and moderately to slightly decomposed granite (MDG/SDG).

Fill is about 22 m thick. It was described as a medium dense, greyish brown and grey, silty fine to coarse SAND with some subangular fine gravel sized rock fragments.

As indicated in the Hong Kong Geological Survey Memoir No. 2 (GCO, 1986) , the site is underlain by two formations of the offshore Marine Deposits: Chek Lap Kok Formation and Hang Hau Formation which are respectively equivalent to the terms Alluvium and Marine Deposits commonly used in the site investigation practice.

Marine Deposits were found in DH2, DH3, DH7, DH8, DH9 and DH10, as shown in Figure 1. Marine Deposits were described as a firm to very stiff, greenish grey, sandy silty CLAY with some shell fragments. Alluvium is thick, in the range of 10 m to 27 m, in the site. It is interbedded with very stiff, greyish brown, slightly sandy SILT, very stiff, dark grey sandy silty CLAY, and very dense, yellowish brown, silty fine to coarse SAND with some subangular fine gravel sized rock fragments

Underlain the alluvium is the residual soil/CDG zone, which is 6 m to 52 m thick in the site. Bedrock of MDG/SDG is found at about 50 m below ground.

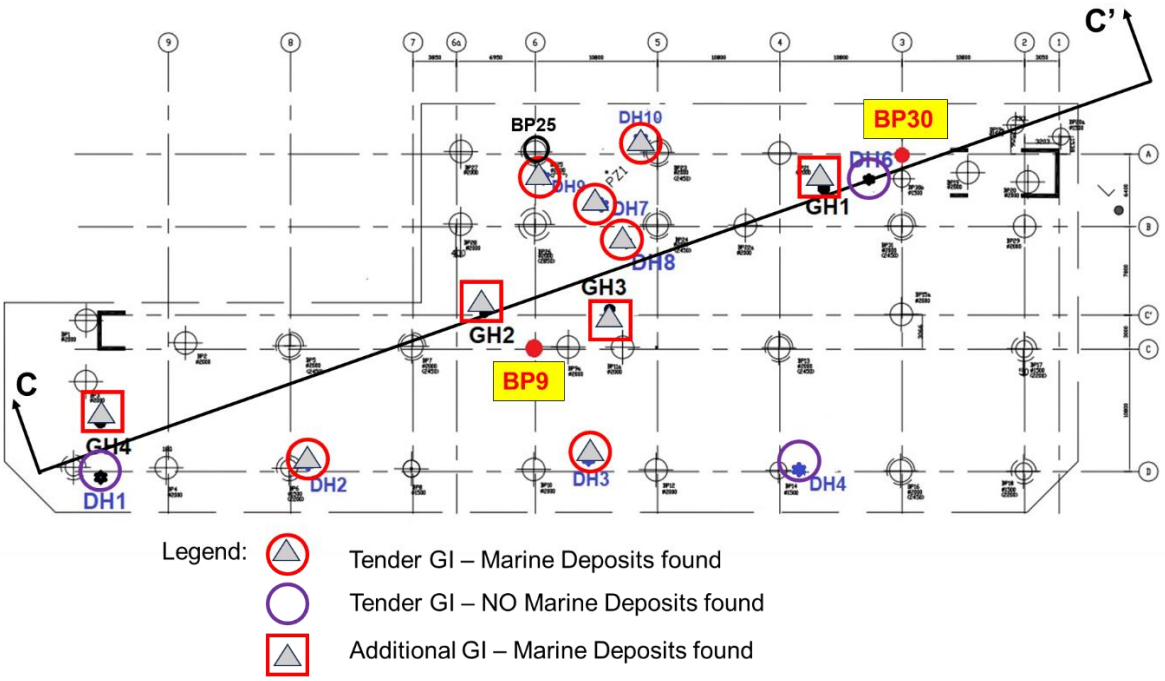


Figure 1: Location of Tender and Additional GI Drillholes

Proceedings DOI: 10.21467/proceedings.8.2
ISBN: 978-81-688301-1-0

Series: AIJR Proceedings
ISSN: 2582-3922

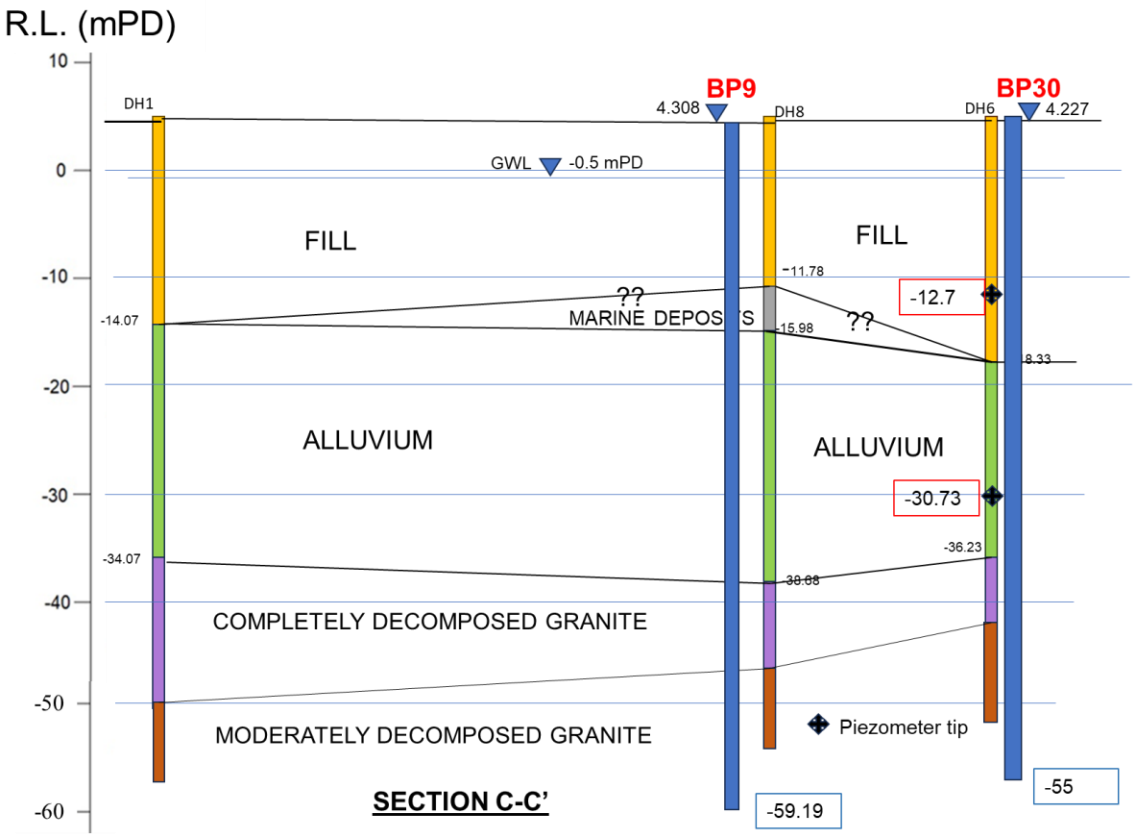


Figure 2: Geological Profile of the Site based on Tender GI information

2.2 Groundwater Conditions

Piezometers/standpipes were installed in DH6 and DH7. The tips of the piezometers/standpipes were located in fill and alluvium. The levels at which the tips were installed in DH6 are included in Figure 2.

The GWL recorded was steady with no marked fluctuation. At DH6, GWL was at -1.0 mPD to -1.2 mPD, at about 5.3 m below ground. At DH7, GWL was at -1.3 mPD to -0.3 mPD, at about 5.0 m below ground.

3 CONCRETING PROBLEM

3.1 Concreting Problem in BP30

BP30 is a 2 m diameter pile founded at -55 mPD with a 2 m rock socket. It has no bell-out. At this pile location, the ground level is at 4.227 mPD. In all, a total of 8 lengths of casing up to 59.14 m long were installed, and the final casing toe level was at -52.91 mPD.

After the 29th truck concrete pour of 217.4 m^3, the casing toe level was lifted by 600 mm from -25.123 mPD to -24.523 mPD. The concrete level in the casing dropped suddenly by 4.7 m from -10.673 mPD to -15.373 mPD, as shown in Figure 3.

Another 5 loads of concrete of 37.5 m^3 (30th to 34th truck) were added, followed by lifting of the casing. The concrete level failed to rise. A further length of the casing was extracted, lifting the casing toe level to -21.663 mPD. The concrete level became -12.773 mPD.

The concrete overflew when the tremie pipe was cut after the 34th truck concrete pour. It was not possible to re-insert the tremie pipe through the hardened concrete layer at -12.773 mPD. It was suspected that there was a hardened concrete layer from -12.773 mPD down to the casing toe level of -24.523 mPD where the casing toe level was lifted.

As compared with the theoretical volume of concrete, there was a huge increase in the actual concrete volume used at the casing toe level between -41.033 mPD and -25.123 mPD. On completion of the 34th concrete pour,

254.9 m^3 of concrete was used giving an overbreak of 92.14%, and a 28.36 m long casing with the casing toe at -21.633 mPD was left in. The pile was abandoned.

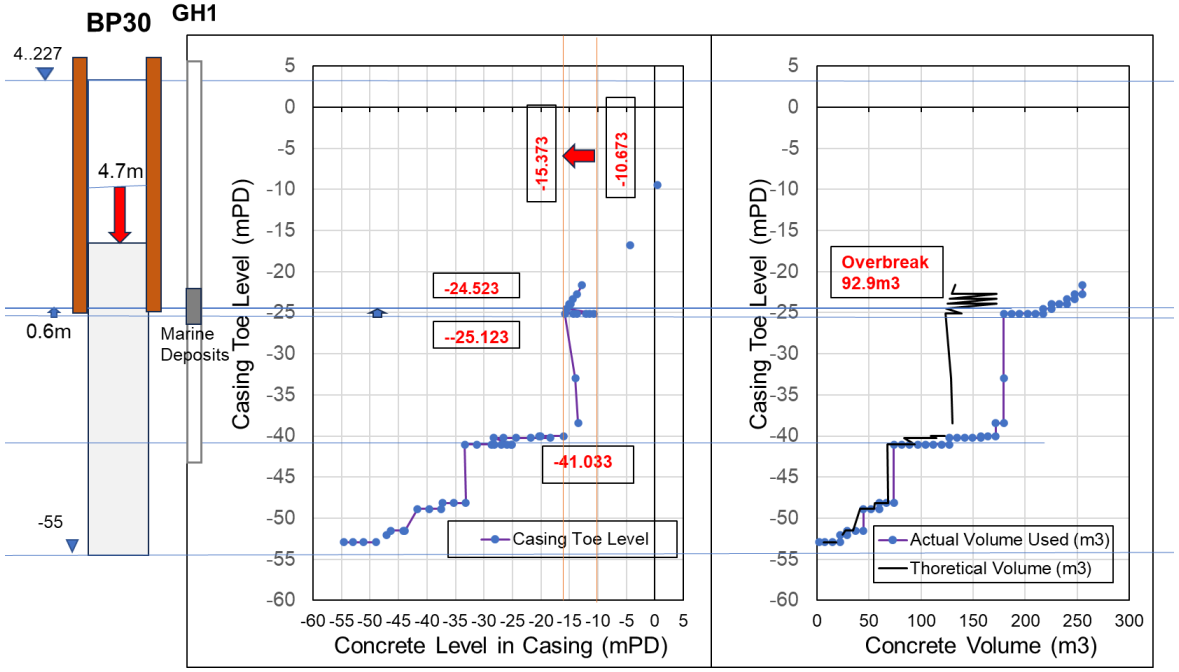


Figure 3: Concreting Records of BP30

3.2 Concreting Problem in BP9

BP9 is a 2 m diameter pile founded at -59.19 mPD with a 2 m rock socket. It has a bell-out of 2.85 m. At this pile location, the ground level is at 4.308 mPD. In all, a total of 8 lengths of casing up to 56.03 m long were installed, and the final casing toe level was at -47.122 mPD.

After the 22nd truck concrete pour of 154 m^3, the casing toe level was lifted by 13.75 m from -37.472 mPD to -23.722 mPD. The concrete level in the casing dropped by 6.5 m from -14.792 mPD to -21.292 mPD, as shown in Figure 4.

There was difficulty to re-insert the tremie pipe into the concrete at -23.722 mPD to continue the concreting. It was suspected that there was a hardened concrete layer at -23.722 mPD.

Another 4 loads of concrete of 28 m^3 (23rd to 26th truck) were added, followed by lifting of the casing toe to -23.122 mPD. The concrete level did not rise. Another 2 loads of concrete of 14 m^3 (27th to 28th truck) were added, followed by lifting of the casing toe to -21.922 mPD. The concrete level rose by 300 mm only to -20.992 mPD. Another 11 loads of concrete of 77 m^3 (29th to 39th truck) were added. The concrete level rose by 20.10 m to 2.308 mPD.

As compared with the theoretical volume of concrete, there was a huge increase in the concrete volume used at the casing toe level between -37.472 mPD and -23.722 mPD. On completion of the concrete pour, 273.0 m^3 of concrete was used giving an overbreak of 44.15%, and a 30.83 m long casing with the casing toe at -21.922 mPD was left in. The pile was subsequently abandoned after widespread concrete defects were found between -21 mPD and -23 mPD (where the Marine Deposits were found (see Figure 5)) by sonic logging and in the samples retrieved from the investigation coring,

4 ADDITIONAL GI WORKS

The objective of the additional GI works was to establish if there was any significant variation in the ground and groundwater conditions at the BP30 and BP9 locations which could give rise to the concreting problem in the piles. A total of 4 additional drillholes (GH1, GH2, GH3 and GH4) were completed. Two VW piezometers with one each in fill and alluvium were installed in GH2, GH3 and GH4. The data from the piezometers were collected by wireless dataloggers and transmitted by long range radio to a data server embedded in the gateway (see Figure 7) . Location of these drillholes is included in Figure 1. The geological profile of the site based on

Proceedings DOI: 10.21467/proceedings.8.2
ISBN: 978-81-688301-1-0

Series: AIJR Proceedings
ISSN: 2582-3922

the additional GI information along Section C-C' is shown in Figure 5. The levels at which the VW piezometers were installed are also included.

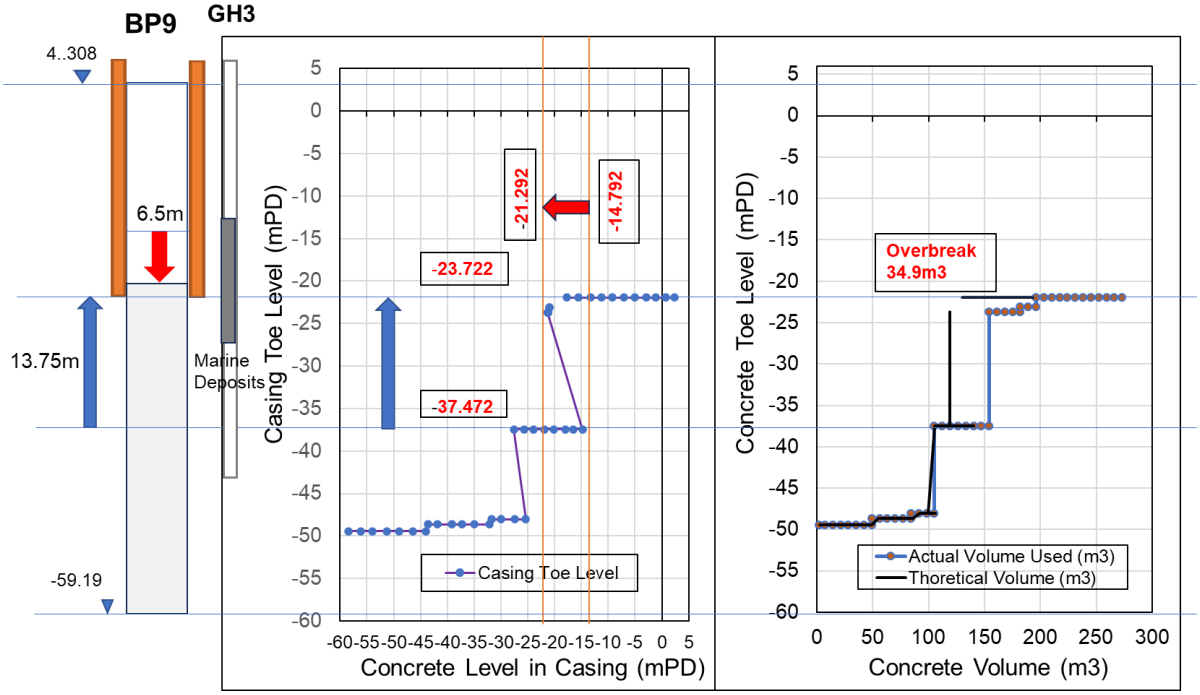


Figure 4: Concreting Records of BP9

5 FINDINGS OF ADDITIONAL GI WORKS

5.1 Greater Extent and Thickness of Marine Deposits at BP30 and BP9 Locations

Marine Deposits were found in all additional drillholes (GH1 to GH4). The extent and thickness of the Marine Deposits at the BP30 and BP9 locations were more substantial than those indicated in the tender GI information.

GH1 was close to BP30, and GH3 to BP9. The tender GI drillholes close to GH1 and GH3 were DH6 and DH8 respectively. At GH1, there was a 3 m thick Marine Deposits, but no Marine Deposits were found at DH6. Marine Deposits were 14 m thick at GH3, but 4.5 m thick at DH8.

There were Marine Deposits at the casing toe level of -24.523 mPD and -23.722 mPD in BP30 and BP9 respectively at which the concreting problem occurred.

Marine Deposits were also found in GH4 and GH2: 6.2 m thick at GH4 and 2.5 m thick at GH2. In between GH2 and GH3, the thickness of the Marine Deposits increased from 2.5 m to 14 m.

It is noted in GCO (1986) that Marine Deposits of the Hang Hau Formation could go up to 20 m thick.

5.2 Weaker and More Compressible Marine Deposits at BP30 and BP9 Locations

A comparison of the SPT N values of Marine Deposits between those indicated in the tender and additional GI works is given in Figure 6.

The SPT N values of Marine Deposits taken in the tender GI works were significantly higher than those taken in the additional GI works. An average SPT N value of 23.3 and 8 was obtained from the tender and additional GI works respectively. At -20 mPD, the SPT N value was found to be 23 from the tender GI works and 8 from the additional GI works. The Marine Deposits encountered were weaker and more compressible, as compared with those shown in the tender GI works.

5.3 Strong Tidal Fluctuation of Groundwater Level

There was a strong tidal fluctuation of groundwater level at the site. Typical plots of the groundwater levels recorded by the VW piezometers PZ2b in fill and PZ2a in alluvium in GH2 are shown in Figure 7. There was a tidal fluctuation of over 1.5 m/day and 2 m/day for the groundwater in fill and alluvium.

This tidal fluctuation of groundwater could lead to a significant loss in soil strength from its initial value (Ke & Takahashi, 2012), in particular for the weaker Marine Deposits at BP30 and BP9.

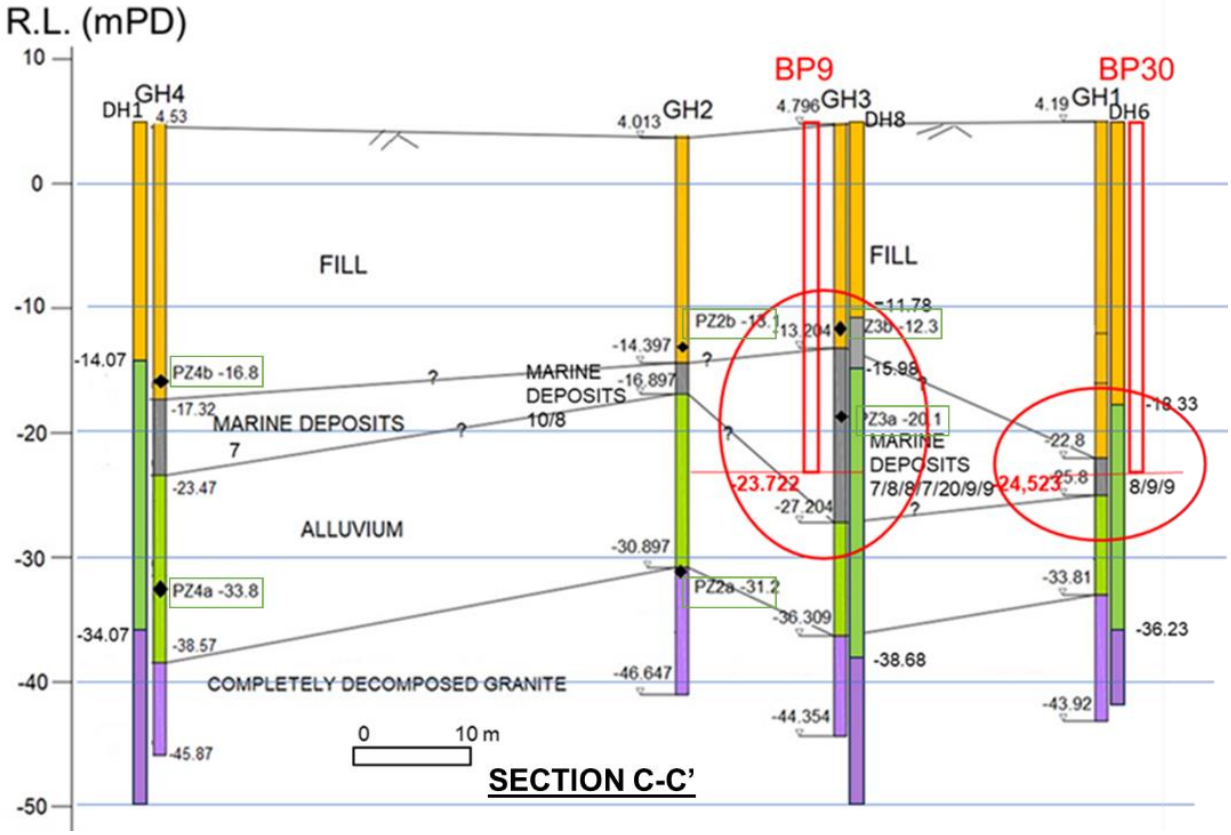


Figure 5: Geological Profile of the Site based on Additional GI information

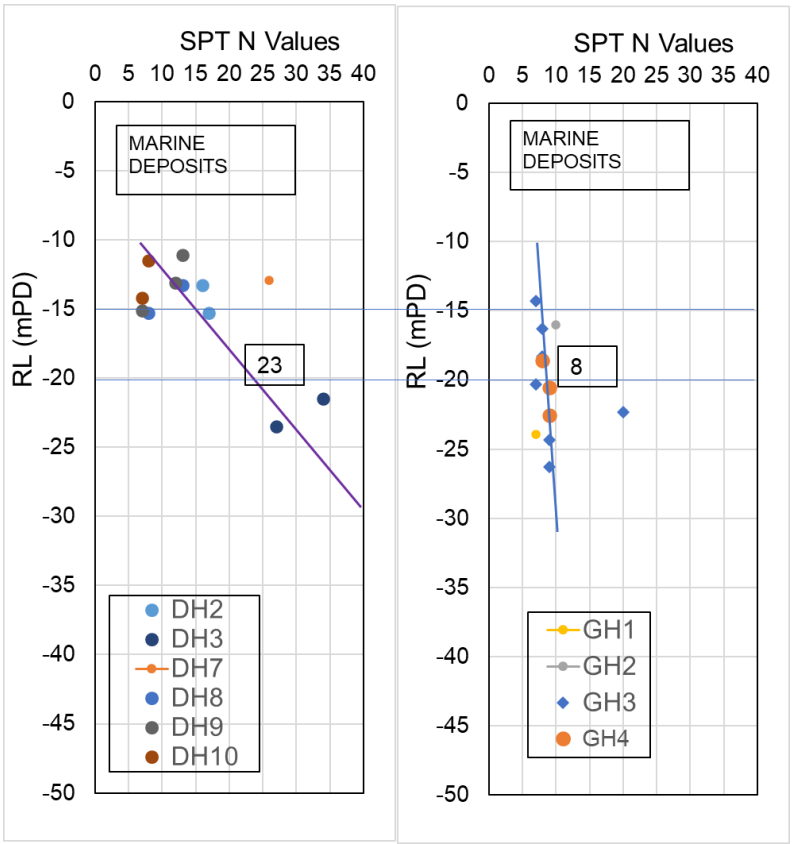


Figure 6: Plot of SPT N Values Between Tender and Additional GI Works

Proceedings DOI: 10.21467/proceedings.8.2
ISBN: 978-81-688301-1-0

Series: AIJR Proceedings
ISSN: 2582-3922

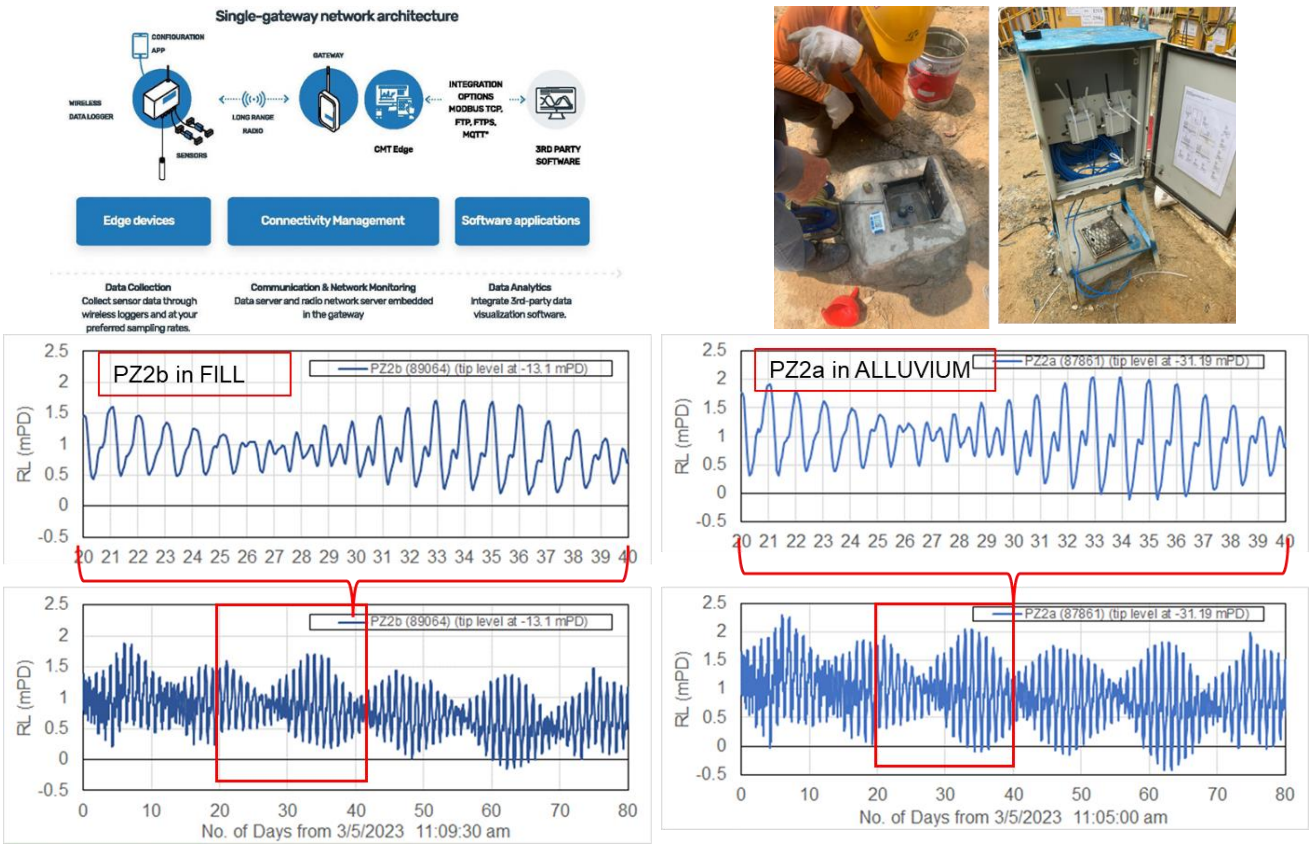


Figure 7: Typical Plot of Groundwater Levels at PZb and PZa at GH2

6 INVESTIGATION

The objective of the investigation was to gather evidence to support the mechanism postulated for the early setting of concrete, and hence the formation of a hardened concrete layer. This was achieved by examination of (i) the composition and contents of the contaminated concrete in the piles; (ii) the effect of Marine Deposits on the early setting of concrete, and (iii) other ambient factors, such as presence of dissolved CO_2 in groundwater and organic matter in Marine Deposits that could favour the process of early setting of concrete.

An investigation drillhole (C3) had been taken at the centre of BP30 upon completion of the concreting. The cement grout/concrete samples retrieved from C3 at -5.891 mPD and -7.94 mPD were sent for PSD, XRD and XRF tests. The tests were carried out by the Hong Kong Polytechnic University.

Water samples from a nearby pile (BP25) (see Figure 1) were taken at -24 mPD and -28 mPD and sent for testing of dissolved CO_2 content. The tests were carried out by Fugro Technical Services Ltd. and SGS Hong Kong Ltd. Soil samples of Marine Deposits retrieved from GH4 were tested for organic matter content. The tests were carried out by ETS-Testconsult Limited.

7 FINDINGS OF THE INVESTIGATION

7.1 Presence of Clay Minerals in Contaminated Concrete

A summary of the PSD, XRD and XRF test results is given in Tables 1 and 2. Typical plot of the XRD test results is given in Figure 8.

There was some 3% clay in the samples from the PSD tests, and 0.53% to 2.88% from the XRD tests, which confirmed the ingress of Marine Deposits into BP30. The clay minerals are represented by illite and kaolinite.

The presence of clay in the wet concrete has a detrimental effect on the concrete. The clay absorbed water from the wet concrete to form a paste, resulting in loss in workability and early setting of concrete.

The effects of clay on the concrete properties had been investigated by Elahi & Ali (2017). The results of the studies showed that there was a drastic loss in the slump values of concrete as the clay content in the concrete increased. A loss in the slump values from 14% to 64% up to a clay content of 6% was measured. Similar studies were carried out by Choudhary et. al. (2019). In this case, the slump value decreased from 140 mm to 125 mm, as the clay content was increased to 2%.

7.2 Presence of Calcium Carbonate in Contaminated Concrete

In the hydration (setting) of concrete, the main components of cement (alite (C_3S) and belite (C_2S)) react with water to form new compounds, including calcium silicate hydroxide (C-S-H) and calcium hydroxide ($Ca(OH)_2$), as shown in Table 3.

As seen in Table 2, there is some 68.26% to 69.77% of calcium carbonate ($CaCO_3$) in the samples as revealed by the XRD tests, and 26.15% to 51.14% by the XRF tests. A slight difference in the percentage of $CaCO_3$ was found between the XRD and XRF tests because different samples were involved. $CaCO_3$ is represented by calcite and vaterite (which is a polymorph of $CaCO_3$).

Apophyllite, which is a potassium-calcium-fluoride silicate mineral, was also found in the XFD/XRF tests, which represented the C-S-H.

The formation of C-S-H and $CaCO_3$ led to the early setting of concrete, and hence the formation of a hardened concrete layer in BP30.

7.3 Presence of Dissolved CO_2 in Groundwater and Organic Matter in Marine Deposits

It was found that there was some 5 to 8% mg/L dissolved CO_2 in groundwater and some 0.1% organic matter in Marine Deposits. CO_2 enhances early setting of concrete. With CO_2, further carbonation reactions of C_3S and C_2S (the cement components of the wet concrete) took place forming $CaCO_3$ and C-S-H, as follows:

$$C_3S + CO_2 + H_2O \rightarrow \text{C-S-H} + H_2O + CaCO_3 \quad (1)$$

$$C_2S + CO_2 + H_2O \rightarrow \text{C-S-H} + H_2O + CaCO_3 \quad (2)$$

Presence of CO_2 can produce a rapid strength gain in concrete (Khan et. al., 2018). Monkman et. al. (2016) in their tests using CO_2 as an accelerating admixture to concrete found that the reaction between CO_2 and the hydrating cement created finely distributed $CaCO_3$ that influenced the subsequent hydration. It was found that for the concrete batch with the CO_2 injection, the time to initial set and final set was reduced by an average 25% and 23% respectively with respect to the batch without the CO_2 injection.

The organic matter in Marine Deposits produced CO_2 which helps facilitate the process of early setting of concrete.

Table 1: Summary of PSD Test Results for Samples from Drillhole C3 in BP30

PSD by weight				
Sample	Clay	Silt	Sand	Gravel
at -5.891 mPD	3%	50%	47%	0%
at -7.94 mPD	0%	10%	90%	0%

Proceedings DOI: 10.21467/proceedings.8.2
ISBN: 978-81-688301-1-0

Series: AIJR Proceedings
ISSN: 2582-3922

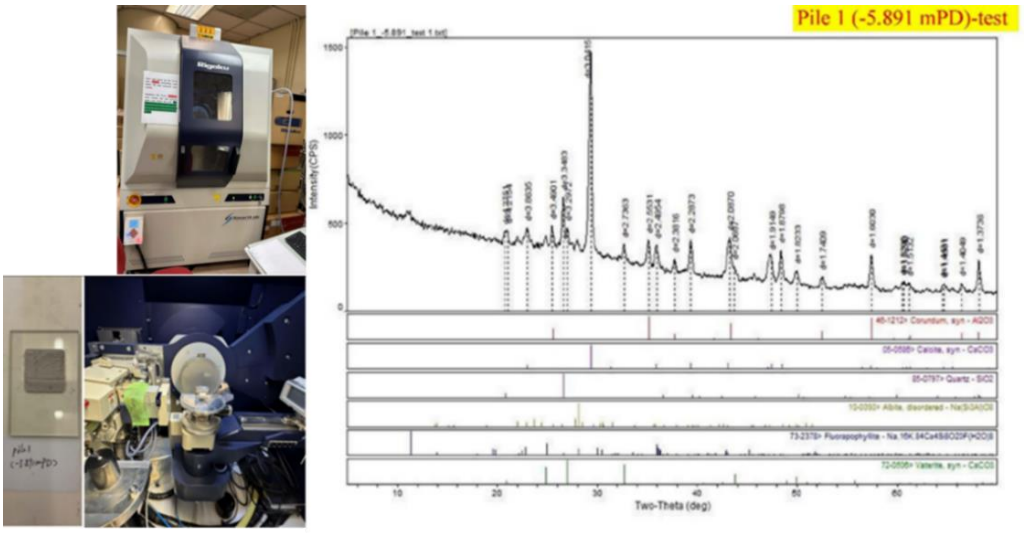
Table 2: Summary of XRD and XRF Test Results for Samples from Drillhole C3 in BP30

Mineral	Description	Samples at -5.891 mPD (% by weight)	Samples at -7.94 mPD (% by weight)
Apophyllite	a potassium-calcium fluoride-silicate mineral	1.26%	7.69%
Illite	a clay mineral	1.99%	0.53%
Kaolinite	a clay mineral	0.89%	0.00%
Albite	a plagioclase feldspar mineral	12.33%	4.15%
Calcite	calcium carbonate ($CaCO_3$)	48.20%	62.60%
Vaterite	a polymorph of calcium carbonate ($CaCO_3$)	21.57%	5.36%
Quartz	an essential mineral in granites, granodiorites & rhyolites	13.76%	19.67%
		100.00%	100.00%

XRD

Mineral	Description	Samples at -5.891 mPD (% by weight)	Samples at -7.94 mPD (% by weight)
Apophyllite	a potassium-calcium fluoride-silicate mineral	1.70%	1.68%
Amorphous		21.24%	18.03%
Microcline	an igneous rock-forming tectosilicate mineral	3.53%	0.00%
Albite	a plagioclase feldspar mineral	13.31%	37.23%
Calcite	calcium carbonate ($CaCO_3$)	44.47%	24.48%
Vaterite	a polymorph of calcium carbonate ($CaCO_3$)	6.67%	1.67%
Quartz	an essential mineral in granites, granodiorites & rhyolites	9.07%	16.91%
		100.00%	100.00%

XRF



(a) Equipment Used (b) X-ray Diffraction Plot

Figure 8: Typical X-ray Diffraction Test Result

.

Table 3: Hydration of Cement

Ordinary Portland Cement (OPC)					Concrete		
Chemical Compounds			% (by weight)		Chemical Compounds		% (by weight)
	Chemical Formula				Calcium Silicate Hydrate	C-S-H	48%
Alite	$3CaO.SiO_2$	C_3S	70%	Hydration	Calcium Hydroxide	$Ca(OH)_2$	14%
Belite	$2CaO.SiO_2$	C_2S	15%	→	Ettringite	Aft (ett)	4%
Aluminate	$3CaO.Al_2O_3$	C_3A	8%		Hydrated Calcium Aluminate	Afm	11%
Ferrite	$4CaO.Al_2O_3.Fe_2O_3$	C_4AF	7%			Anhyd	3%
						Pores	16%
						Other	4%

8 MECHANISM OF CONCRETE CONTAMINATION BY MARINE DEPOSITS IN BP30 AND BP9

The mechanism that took place in BP30 and BP9 leading to the concreting problem is postulated, as follows:

8.1 Turbulent flow of Wet Concrete Down the Casing Upon Lifting of the Casing

The downward flow of wet concrete in the casing is like a flow through a sudden expansion in a pipe, as shown in Figure 9(a), except that the flow is vertically downwards.

Reynolds number (Re) was used to assess the nature of flow. Re is a dimensionless number given by the ratio of inertia force to viscous force, as follows:

$$R_e = \frac{\rho v D}{\mu} \tag{3}$$

where ρ is the density of the fluid (kg/m^3); v is the flow speed (m/s); D is a characteristic linear dimension (m) and μ is the dynamic viscosity of the fluid (Pa·s, N·s/m^2 or kg/(m·s)).

When Re is less than 2000, the flow is laminar. If Re is greater than 3500, the flow is turbulent. When Re lies between 2000 and 3500, the flow is a transitional flow. In laminar flow, viscous forces are dominant, and fluids move along smooth streamlines. In turbulent flow, inertial forces dominate and tend to produce chaotic eddies, vortices and other flow instabilities. A comparison of the flow pattern of laminar flow and turbulent flow is shown in Figure 9(b). In the figure, the straight, parallel black lines are streamlines which are parallel to the mean flow (streamlines). In laminar flow, the fluid particles follow the streamlines. In turbulent flow, eddies of different sizes are superimposed onto the mean flow, and in the turbulent region, the flow follows both the mean flow and the eddies. Larger eddies cause lateral flow across streamlines, and small eddies create smaller scale stirring that causes the flow to spread (diffuse).

There was a rapid change in head as the wet concrete flowed downwards. The change in head of the wet concrete before and after lifting of the casing can be represented by the Bernoulli's equation, assuming that the wet concrete is an incompressible, frictionless fluid, as follows:

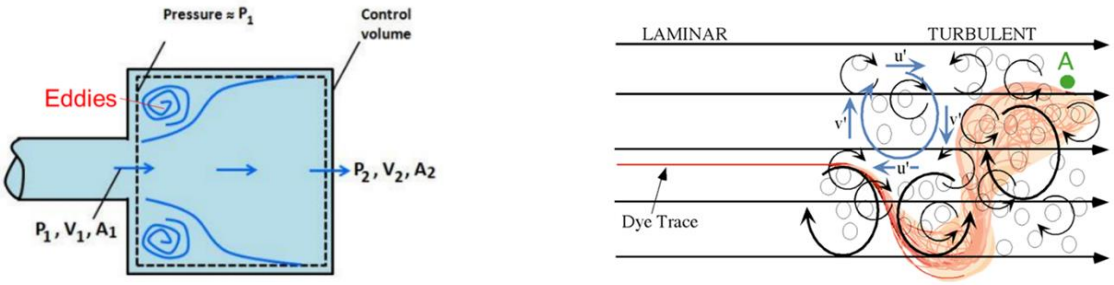
$$P + \frac{1}{2}\rho v^2 + \rho g h = constant \tag{4}$$

$$\frac{P}{\rho g} + \frac{v^2}{2g} + h = constant \tag{5}$$

where P = Pressure head = pressure energy per unit volume; V = Velocity head = $\frac{1}{2}\rho v^2$ = kinetic energy per unit volume and Z = Elevation head = ρgh = potential energy per unit volume

Applying Equation (5) to the flow conditions before and after lifting of the casing toe level from -25.123 mPD to -24.523 mPD for BP30, and from -37.472 mPD to -23.722 mPD for BP9 (see Figures 3 and 4), the Re for the downward flow of the wet concrete was calculated. The typical parameters used in the evaluation of the Re for BP9 are given in Figure 10. In the evaluation, a density of 2600 kg/m^3 and a dynamic viscosity of 25 Pa.s were used for the wet concrete (see Ferraris (1999)).

The Re for the downward flow of the wet concrete was found to be 5365 for BP30 and 2121 for BP9, which indicates that the flow of the wet concrete in BP30 was fully turbulent, whereas the flow in BP9 was transitional. The diameter of the bulged diameter of BP30 developed was calculated to be 5.9 m, as compared with 2.4 m in BP9. The downward velocity of the flow of the wet concrete was calculated to be about 8.5 m/s in both cases.



(a) Flow through a Sudden Expansion in a Pipe (b) Flow Pattern of Laminar and Turbulent Flow

Figure 9: Characteristics of Laminar and Turbulent Flow

Proceedings DOI: 10.21467/proceedings.8.2
ISBN: 978-81-688301-1-0

Series: AIJR Proceedings
ISSN: 2582-3922

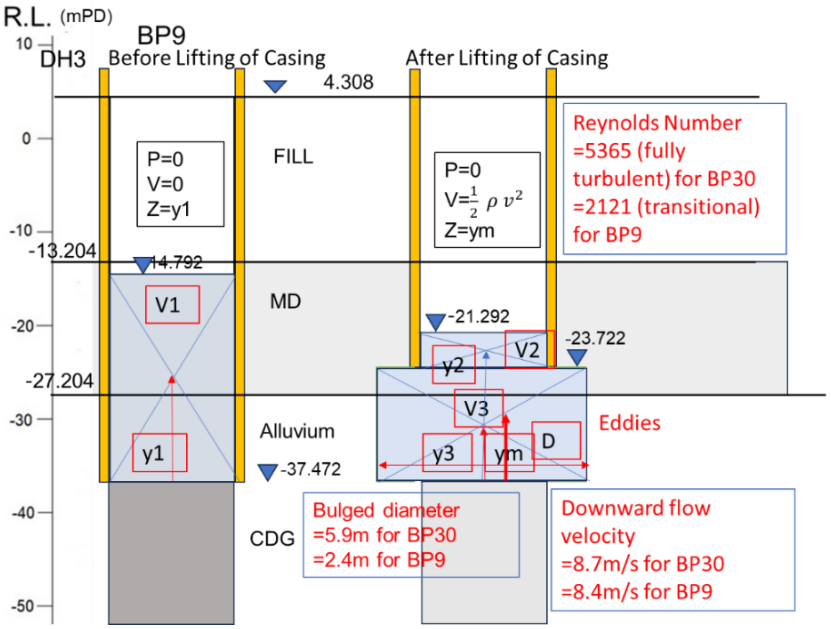


Figure 10: Parameters Used in the Evaluation of Reynolds Number

8.2 Base Heave Failure and Squeezing Out of Marine Deposits by Wet Concrete at the Casing Toe Level

There was base heave failure during shaft excavation in BP30 and BP9. The factor of safety (FS) for base heave for BP30 and BP9 at 27.3 m depth (=25.8m-2m+4.3m, where the 2 m is the height of the soil above the casing toe) and 29.507 m depth (=27.204m-2m+4.3m) respectively (which correspond closely to the depths at which the concreting problem occurred in the piles) was used and computed using Equation (6) (the method by Bjerrum and Eide (1956)).

$$FS = \frac{C_u N_c}{\gamma H} \tag{6}$$

where Cu = undrained shear strength (kPa); Nc = bearing capacity factor; γ = unit weight of soil (kN/m^3) and H = depth to excavation (m).

In the evaluation, a SPT N value of 8, as that obtained from the additional GI works at -20 mPD, was used. This gives an unconfined compressive strength (qu) of 50 kPa to 100 kPa or a Cu of 75/2 = 37.5 kPa, corresponding to a medium stiff CLAY (see Das (2007)).

The FS for base heave was found to be less than 1 in both cases.

For BP30, given H = 27.3 m, L/B = 1 and H/B > 4, Nc becomes 9 (see Bjerrum and Eide (1956)). Using an average γ of 18 kN/m^3, the FS for base heave was 0.687, as shown below:

$$FS = \frac{C_u N_c}{\gamma H} = \frac{37.5x9}{18x27.3} = 0.687 \lll 1 \ (failure) \tag{7}$$

For BP9, H is 29.507 m. The FS for base heave was 0.635, as shown below:

$$FS = \frac{C_u N_c}{\gamma H} = \frac{37.5x9}{18x29.507} = 0.635 \lll 1 \ (failure) \tag{8}$$

With the base heave failure occurring, Marine Deposits outside the casing flew into the casing creating cavities outside the casing, as the Marine Deposits inside the casing were excavated.

Upon lifting of the casing toe level from -25.123 mPD to -24.523 mPD for BP30, and from -37.472 mPD to -23.722 mPD for BP9, the wet concrete flew down the casing, pushed the Marine Deposits outwards and squeezed into the cavities inside the Marine Deposits. Based on the concrete placement records, the overbreak for this portion of the pile was 74.63% for BP30 and 29.35% for BP9, with the diameter increasing from 2 m to 5.9 m for BP30 and to 2.4 m for BP9 respectively (see Section 8.1).

It should be noted that if a SPT N value of 23 was used, as that obtained from the tender GI works at -20 mPD, a qu of 200 kPa to 400 kPa or a Cu of 300/2=150 kPa, corresponding to a very stiff CLAY, would be obtained. This would give a FS for base heave of 2.747 and 2.542 for BP30 and BP9 respectively, implying that base heave in the piles would not occur.

8.3 Turbulent Mixing and Contamination of Wet Concrete by Marine Deposits in particular at the Casing Toe Area

The flow of the wet concrete down the casing in BP30 was fully turbulent. The flow produced eddies and vortices which caused ingress of the Marine Deposits and turbulent mixing and contamination with the wet concrete, in particular near the casing toe area. The flow in BP9 was a transitional flow. Some eddies and vortices were developed causing minor ingress of Marine Deposits and mixing with the wet concrete. Hence, the ingress of Marine Deposits into the wet concrete, and the concreting problem, was less serious in BP9 than in BP30.

8.4 Early Setting of Concrete Forming a Hardened Concrete Layer

The Marine Deposits, which contained clay and dissolved CO_2, contaminated the wet concrete and triggered the early setting of the concrete forming a hardened concrete layer. The dissolved CO_2 in groundwater and organic matter in Marine Deposits provide a good environment for the early setting of concrete. The tidal fluctuation of groundwater helped recharge CO_2 in groundwater and organic matter in Marine Deposits and further facilitate the process of early setting of concrete.

9 CONCLUSIONS

The following conclusions can be made from the study:

(a) The concreting problem that had occurred in BP30 and BP9 was not the result of a single event, but a combination of different latent conditions that had stacked up to produce the major defect (like a Swiss Cheese Model incident). The latent conditions are defined as hidden, unexpected physical or systemic issues (like subsurface rock, contaminated soil, or design flaws) that are not reasonably discoverable during initial site inspections or tendering but emerge during the works, causing extra costs or delays. They represent pre-existing weaknesses that lie dormant until triggered, leading to failures or adverse outcomes, especially in construction, engineering, and safety. In this case, the latent conditions included the presence of an unexpected layer of thicker and weaker Marine Deposits at the pile locations, strong tidal fluctuation of groundwater (which weakened the soils), and presence of dissolved CO_2 in groundwater and organic matter in Marine Deposits (which provided a favourable condition for the occurrence of the problem).

(b) The mechanism for the concreting problem in BP30 and BP9 was complicated involving (i) turbulent flow of wet concrete down the casing upon lifting of the casing; (ii) base heave failure and squeezing out of Marine Deposits by wet concrete at the casing toe level; (iii) turbulent mixing and contamination of wet concrete by Marine Deposits in particular at the casing toe area; and eventually (iv) early setting of concrete forming a hardened concrete layer. The new information obtained by the additional GI works and the investigation provided good support for the mechanism postulated.

ACKNOWLEDGEMENTS

The author would like to thank Wilson & Associates Limited for the support and permission to publish the paper. Thanks are also due to Professor J.H. Yin of the Hong Kong Polytechnic University for reviewing the investigation report and supervising the PSD, XRD and XRF tests for the study.

PUBLISHER'S NOTE

AIJR remains neutral with regard to jurisdictional claims in published maps & institutional affiliations.

REFERENCES

Bjerrum, L. & Eide, O. (1956). Stability of Strutted Excavations in Clay. Geotechnique, Vol. 6, No. 1. pp. 32-47.

Choudhary, H. Siddiqui, M.A. & Saha, D. (2019). Effect of Clay Fines on Strength and Workability of Concrete. J. of Civil Engineering and Environmental Technology, Vol. 6, Issue 5, July-September, pp 311-315.

Das, B.M. (2007). Principles of Foundation Engineering.

Elahi, A. & Ali, A. (2017). Effects of Clay on properties of Concrete. Resilient Structures and Sustainable Construction.

Ferraris, C. F. (1999). Measurement of the Rheological Properties of High Performance Concrete: State of the Art Report. Vol. 104, No. 5, September–October 1999 Journal of Research of the National Institute of Standards and Technology.

GCO (1986). Hong Kong Geological Survey Memoir No. 2. Geology of Hong Kong Island and Kowloon.

Ke, L. & Takahashi, A. (2012). Strength Reduction of Cohesionless Soil due to Internal Erosion Induced by One-dimensional Upward Seepage Flow. Soils and Foundations 2012:52(4):698-711, The Japanese Geotechnical Society.

Khan, M.T., Saud, K.R., Irfan, K.A. & Ibrahim, S. (2018). Curing of Concrete by Carbon Dioxide. International Research Journal of Engineering and Technology, Volume: 05 Issue: 04.

Monkman, S., MacDonald, M., Doug Hooton, R. & Sandberg, P. (2016). Properties and Durability of Concrete Produced Using CO2 as an Accelerating Admixture. CarbonCure Technologies, 60 Trider Crescent, Dartmouth, NS B3B 1R6, Canada.